Civil, Construction and Environmental Engineering Publications

Civil, Construction and Environmental Engineering

4-2015

Peel resistance of adhesive joints with elastomer–carbon black composite as surface sensing membranes

Wei Zeng
Iowa State University

Weixing Sun
Iowa State University, wxsun@iastate.edu

Nicola Bowler
Iowa State University, nbowler@iastate.edu

See next page for additional authors

Peel resistance of adhesive joints with elastomer–carbon black composite as surface sensing membranes

Abstract

The peel resistance of four adhesives ("J-B Weld" by J-B Weld (adhesive A), 3 M Scotch-Weld DP 125 Gy (adhesive B), Loctite PL Premium (3x) Construction Adhesive (adhesive C), and Henkel Hysol EA9394 (adhesive D)) is investigated for their bonding performance of a styrene-ethylene/butylene-styrene– carbon black (SEBS–CB) composite membrane used in structural health monitoring (SHM) applications. Tests are performed on membrane samples bonded on four common structural materials, namely aluminium, steel, concrete, and fiberglass, to obtain the peel resistance of adhesives. Results show that adhesive B has the highest strength for aluminium, steel, and fiberglass substrates, and that adhesive C has the highest strength for the concrete substrate. The performance is also evaluated versus adhesive cost, a critical variable in SHM applications. Here, adhesive C performed best for all substrates. Lastly, membrane residuals resulting from the peel tests are compared. Tests show that Adhesive B resulted in the highest residual percentage for aluminium, while adhesive C performed better for all other substrates. However, membrane residuals for adhesive C do not show a positive correlation with the peel resistance.

Disciplines

Civil Engineering | Materials Science and Engineering | Structural Materials | VLSI and Circuits, Embedded and Hardware Systems

Authors

Wei Zeng, Weixing Sun, Nicola Bowler, and Simon Laflamme

Peel Resistance of Adhesive Joints with Elastomer-Carbon Black Composite as Surface Sensing Membranes

Wei Zeng[a], Weixing Sun[b,*], Nicola Bowler[b], and Simon Laflamme[a]

[a]Department of Civil, Construction, and Environmental Engineering, Iowa State University, Ames, IA, 50011

[b]Department of Material Sciences and Engineering, Iowa State University, Ames, IA, 50011

*Corresponding author. Tel: +1 515 294 3933;
Postal address: 3313 Hoover Hall, Materials Science and Engineering, Iowa State University, Ames, IA 50011 USA
E-mail: wxsun@iastate.edu (W. Sun)

Abstract

The peel resistance of four adhesives ("J-B Weld" by J-B Weld (adhesive A) , 3M Scotch-Weld DP 125 Gray (adhesive B), Loctite PL Premium (3x) Construction Adhesive (adhesive C), and Henkel Hysol EA9394 (adhesive D)) is investigated for their bonding performance of a styrene-ethylene/butylene-styrene– carbon black (SEBS-CB) composite membrane used in structural health monitoring (SHM) applications. Tests are performed on membrane samples bonded on four common structural materials, namely aluminium, steel, concrete, and fiberglass, to obtain the peel resistance of adhesives. Results show that adhesive B has the highest strength for aluminium, steel, and fiberglass substrates, and that adhesive C has the highest strength for the concrete substrate. The performance is also evaluated versus adhesive cost, a critical variable in SHM applications. Here, adhesive C performed best for all substrates. Lastly, membrane residuals resulting from the peel tests are compared. Tests show that Adhesive B resulted in the highest residual percentage for aluminium, while adhesive C performed better for all other substrates. However, membrane residuals for adhesive C do not show a positive correlation with the peel resistance.

Keywords: peel (C), peel strength, SEBS-CB, sensor adhesive

1. Introduction

Structural Health Monitoring (SHM) is the automation of the condition assessment process of structural systems. Many SHM applications are engineered for mesosystems, such as transportation infrastructures [1, 2], energy production structures [3-5], and aerospace systems [6]. To enable SHM of geometrically large systems, various types of sensing membranes or skins have been researched and developed [7-10]. The main characteristic of such technology is the deployment of a local sensing solution over a global system, analogous to biological skins. However, the electrical (e.g., signal) and mechanical (e.g., durability) performance of these systems is highly dependent on the adhesive bonding the membrane onto the monitored substrate.

The authors have recently proposed a sensing skin for SHM of wind turbine blades [11, 12]. The sensor is a soft elastomeric capacitor. Its dielectric is fabricated from a styrene-ethylene/butylene-styrene (SEBS) filled with titania, and sandwiched between two layers of

electrodes consisting of an SEBS-carbon black (CB) mix (SEBS-CB). Once installed, one of the electrode layers (SEBS-CB) is directly deployed onto the monitored surface.

In this paper, the performance of four different adhesives for bonding elastomeric sensor electrodes onto various structural substrates is investigated. Performance of adhesives is a modern area of research due to the growth in the fabrication of composite structures. In particular, researchers have studied the resistance-to-peel strength of adhesives for vehicles and aircraft applications [13-15]. Others have investigated the problem of peel stress [16, 17], and fracture mechanisms of epoxies [18-20]. The adhesives under study in this paper are J-B Weld (adhesive A), 3M Scotch-Weld DP 125 Gray (adhesive B), Loctite PL Premium (3x) Construction Adhesive (adhesive C), and Henkel Hysol EA9394 (adhesive D). The selection was based on experience in prior work, availability, and differences in claimed strength, applications, and curing time. Selected structural substrates are 6061 aluminium, A36 steel, concrete, and fiberglass. They were selected due to their common utilization in structural engineering. The comparison between adhesives is conducted by determining the peel resistance, and evaluating cost versus performance, and analyzing SEBS-CB residuals after peel.

The paper is organized as follows. Section 2 discusses materials and methods for the sensing membrane fabrication, sensing membrane adhesion, and the peel resistance measurements and analysis. Section 3 presents and analyses experimental results, including an analysis of the peel resistance and its correlation with post-peel membrane residuals on different substrates. Section 4 concludes the paper.

2. Material and methods

2.1 Sensing membrane fabrication

Sensing materials were fabricated following a previously established fabrication methodology [1, 11, 21, 22]. Briefly, the SEBS-titania composite dielectric was fabricated using a solution casting method. SEBS pellets were dissolved in toluene, and titania particles (Sachtleben R 320 D) were added and dispersed using sonication. The resulting solution was cast on a 10 cm x 10 cm glass plate and kept at room temperature for 5 days to allow toluene to evaporate. The electrodes were fabricated by mixing CB particles (Printex XE 2-B) into an SEBS solution to produce a conductive paint, which was sprayed onto both surfaces of the dielectric to constitute the sensor. Figure 1(a) shows a picture of the resulting sensor. Figure 1(b) shows a picture of a typical sample cut from the fabricated sensor.
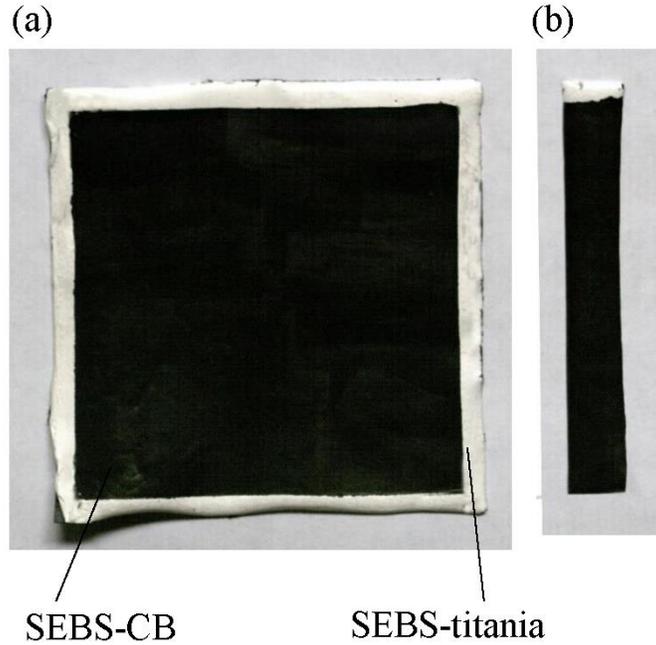
Figure 1 (a) A 10 cm x 10 cm sensing membrane; and (b) a typical 1.3 cm x 9.5 cm sample cut from the fabricated membrane.

2.2 Sensing membrane adhesion

The bonding performance of adhesives was examined for four different substrates: 6061 aluminium plates, A36 steel plates, concrete slabs, and fiberglass sheets, cut into cylindrical shapes of 15 cm diameter and 2.5 cm height (aluminium and concrete), square shapes of 15 cm x 15 cm and 2.5 cm height (steel), and square sheets of 15 cm x 15 cm (fiberglass). Aluminium and steel plates were purchased from Speedy Metals. Concrete slabs were cut from concrete cylinders fabricated using Portland cement and limestone in our lab. Fiberglass sheets were fabricated by structural fiberglass-reinforced polyester (FRP), purchased from McMaster-Carr. The substrates' surfaces are shown in Figure 2(a). Six peel-testing strip samples (each 1.3 cm x 9.5 cm) were cut from each membrane (Figure 1(b)) and adhered onto each substrate. Substrate surfaces were ground using abrasive papers and cleaned with ethanol. A thin layer of adhesive was then smoothly applied on the surface and hand-spread as thin and uniformly as possible. The membrane samples were then deployed by hand onto the adhesives and any air bubbles were gently squeezed out. The mixing and curing procedures of adhesives were based on the commercial instructions given for each adhesive. Figure 2(b) is a schematic of the prepared specimen for a single strip. Approximately 30 mm over one end of the strip was not adhered to allow mechanical attachment of the grip for the peel test. Four different adhesives were selected for testing their bonding performance: adhesive A, adhesive B, adhesive C, and adhesive D. Table 1 lists the main characteristics of each adhesive.

Table 1 Adhesives under study

Adhesives	Adhesive A ("J-B Weld" by J-B Weld)	Adhesive B (3M Scotch-Weld DP 125 Gray)	Adhesive C (Loctite PL Premium (3x) Construction	Adhesive D (Henkel Hysol EA9394)

|				
Price (USD)	7.22	29.59	5.99	23.87
Size	2 oz (57 g) Tube	1.7 oz (48 g) Duo-Pak	10 fl oz (296 mL) Tube	50 mL Dual Cartridge
Cost per ounce (USD)	3.61	17.40	0.60	14.04
Service temperature	-67°F (-55°C) to 550°F (287°C)	-67°F (-55°C) to 180°F (82°C)	0°F (-18°C) to 250°F (121°C)	-67°F (-55°C) to 500°F (260°C)
Water resistance (Y/N)	Y	Y	Y	Y
Curing time at 25°C (78°F)	15 - 24 hours	7 days	24 - 48 hours	3 - 5 days
Application temperature	up to 550°F (288°C)	above 60°F (16°C)	above 40°F (4°C)	close to 77°F (25°C)
Shear strength range (psi)	up to 1040	60 - 3400	33 - 1000	800 - 3500
Recommended use	concrete, fiberglass, metal, and wood	plastics, thermoplastic elastomers, rubber, metal, glass, ceramics, and wood	wood, concrete, stone, granite	potting, filling, and liquid shim materials
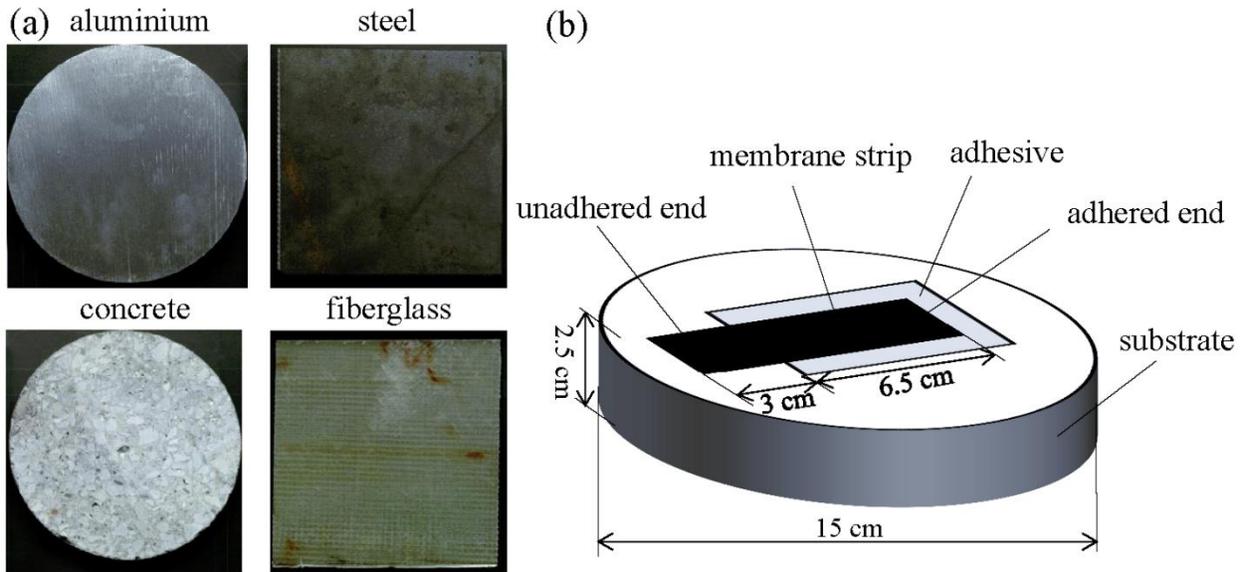
Figure 2 (a) Substrate surfaces; and (b) a schematic of one strip adhered on the substrate.

2.3 Peel test procedures

Peel tests were done to acquire the peel resistance of adhesives by peeling a flexible adherend from a rigid adherend at a 90-degree angle. A single-degree-of-freedom Instron 5569 platform was used to conduct the peel test. Peel tests were initiated at 90 degrees and the angle between

the flexible membrane and the substrate was allowed to vary naturally as the flexible adherend peeled from the rigid adherend. All strip specimens were prepared with the same adhered length and unadhered length (shown in Fig. 2) to ensure the identical peel-angle and comparable data. Tests were conducted at constant rates of extension (peeling rates) at 25 mm/min and 250 mm/min. Figure 3 shows a picture (Figure 3 (a)) and a schematic (Figure 3(b)) of the test setup. A copper tape was used between the grips and the membrane to increase friction. Three strip samples were tested at each peeling rate for each adhesive and each substrate, for a total of 96 tests.
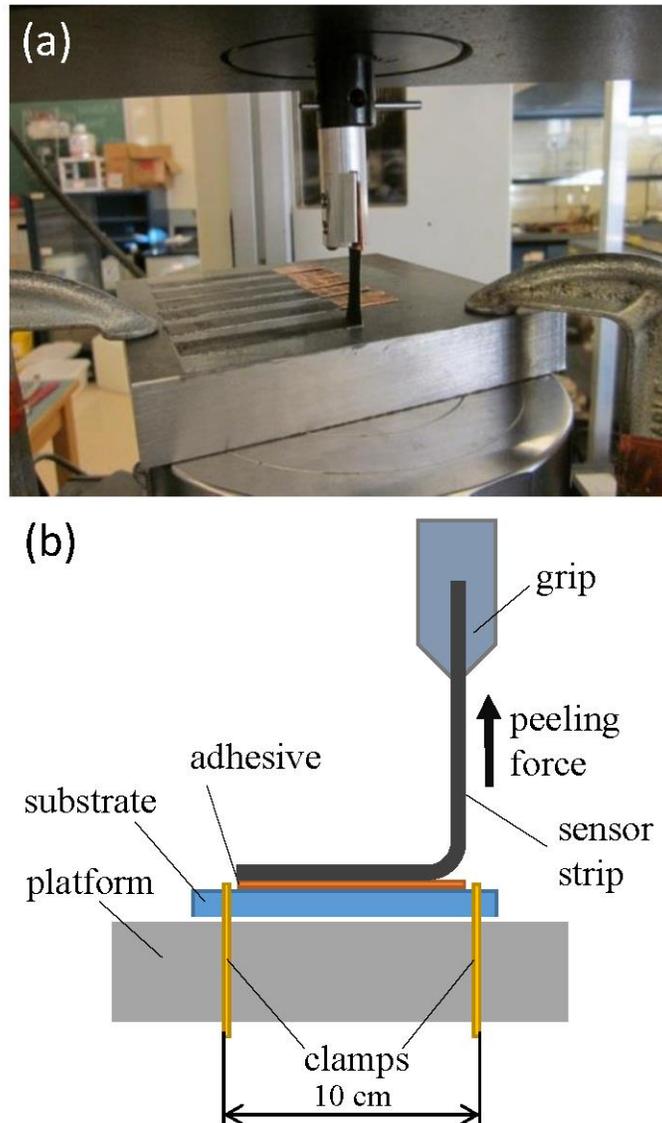
Figure 3(a) A peel resistance test on the Instron 5569 platform; and (b) a schematic of the peel resistance test.

2.4 Analysis of the peel resistance and membrane residuals

The peel resistance was calculated by dividing the peeling force by the specimen width, with units in kN/m. Results are compared using 1) the maximum strength; and 2) the average strength. Data presented shows the average values for all three samples and the standard deviation.

Figure 4 shows a typical result for a peeling test, here using adhesive B on concrete at 250 mm/min peeling rate. As marked on the plot, the maximum strength is taken as the maximum force over the total length of the extension, which typically occurs at the beginning of the test. The average strength is calculated after the first drop in the peeling force. Figure 4 (top) shows that post-peel regions include two parts: a residual SEBS-CB layer (black) and substrate surface regions (light gray). The black colour arises from the SEBS-CB residual that remained on the adhesive. The gray arrows point out the peeled-off areas corresponding to a decrease of peeling force. The percentage of membrane residual after peel was computed by analyzing pixel counts from pictures taken after each test by comparing dark versus light colour areas. Pictures of post-peel regions were processed in black-and-white. The colour index (0 (pure black) - 255 (pure white)) for all pixels was read in each picture and the ratio 'darker colours over the entire post-peel area' was taken as the membrane residual ratio. This computation was done in MATLAB.
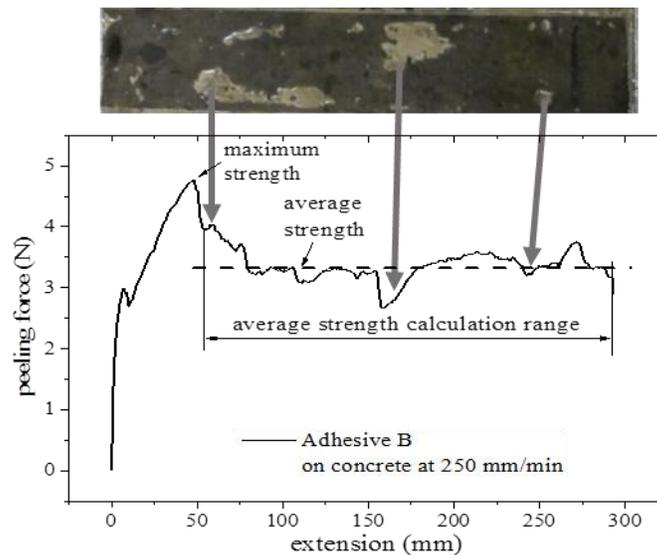

Figure 4 The peeling force as a function of peeling extension (bottom) and corresponding post-peel picture (top) for a typical result.

3. Results and Discussion

3.1 Analysis of the peel resistance

Figure 5 shows the peel resistance of the adhesives on aluminium, steel, concrete, and fiberglass, respectively. Results reveal a positive relationship between the peel resistance and the peeling rate in all 16 data sets on both maximum and average strengths. Furthermore, as shown in Figures 5(a) and 5(b), adhesive B shows the highest average strength on aluminium and steel substrates at both peeling rates, indicating that adhesive B is more suitable for metal substrates compared to other adhesives. Figure 5(c) shows that adhesive C exhibits the best performance for concrete, and Figure 5(d) shows that both adhesive B and adhesive C have similar average strength for fiberglass.
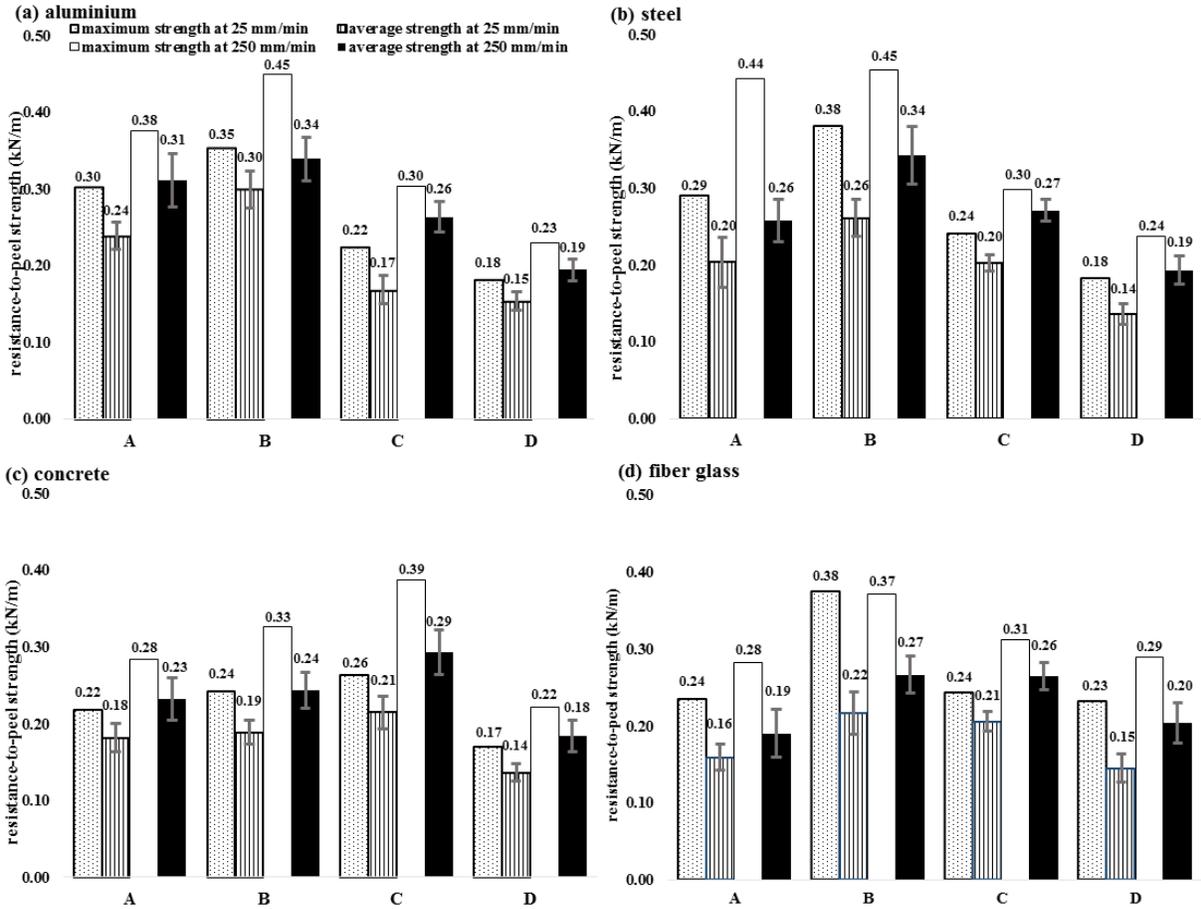
Figure 5 The peel resistance of four adhesives on (a) aluminium, (b) steel, (c) concrete, and (d) fiberglass.

Figure 6 presents the resistance-to-peel strength/USD per ounce (USD per ounce is calculated by the retail price of adhesives divided by the weight), a measure of cost-effectiveness useful for large-scale deployments. While adhesive B obtained superior performance with most substrates for the peel-to-resistance strength, a cost analysis shows low cost-effectiveness for adhesive B. Conversely, adhesive C shows a substantially high cost-effectiveness with respect to other adhesives, making it a good choice for applications in which strength provided by adhesive C (Figure 5) is adequate.
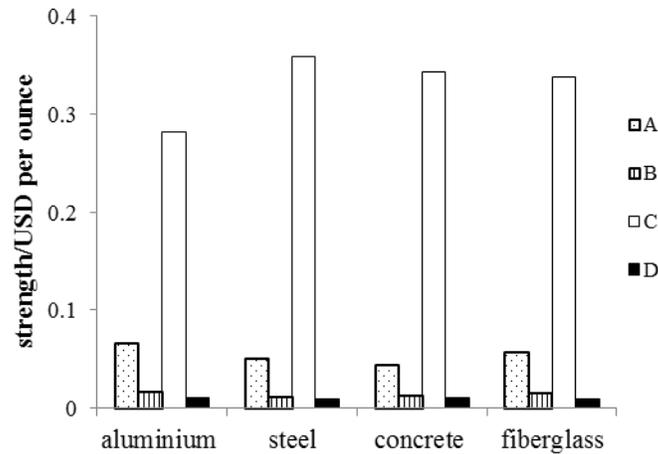
Figure 6 Resistance-to-peel strength/USD per ounce at 25 mm/min peeling rate.

3.2 Analysis of membrane residuals after peel

Figure 7 presents results of the residual percentage of membranes as a function of the resistance-to-peel strength to provide an additional measure of adhesive performance. The residual membrane results from the cohesive substrate failure, i.e., failure of the adherend [23]. Moreover, the peeled membrane is attributed to adhesion failure [23], indicating inferior bonding performance in the area. All adhesives show a positive correlation between the membrane residual and the resistance-to-peel strength, except adhesive C. In other cases, the highest peel resistance corresponds to the highest residual percentage of membranes, consistent with results of similar adhesive tests [24]. However, instead of an opaque or translucent membrane layer with distinct peeled-off regions, adhesive C samples display a very thin and transparent layer on all substrates.
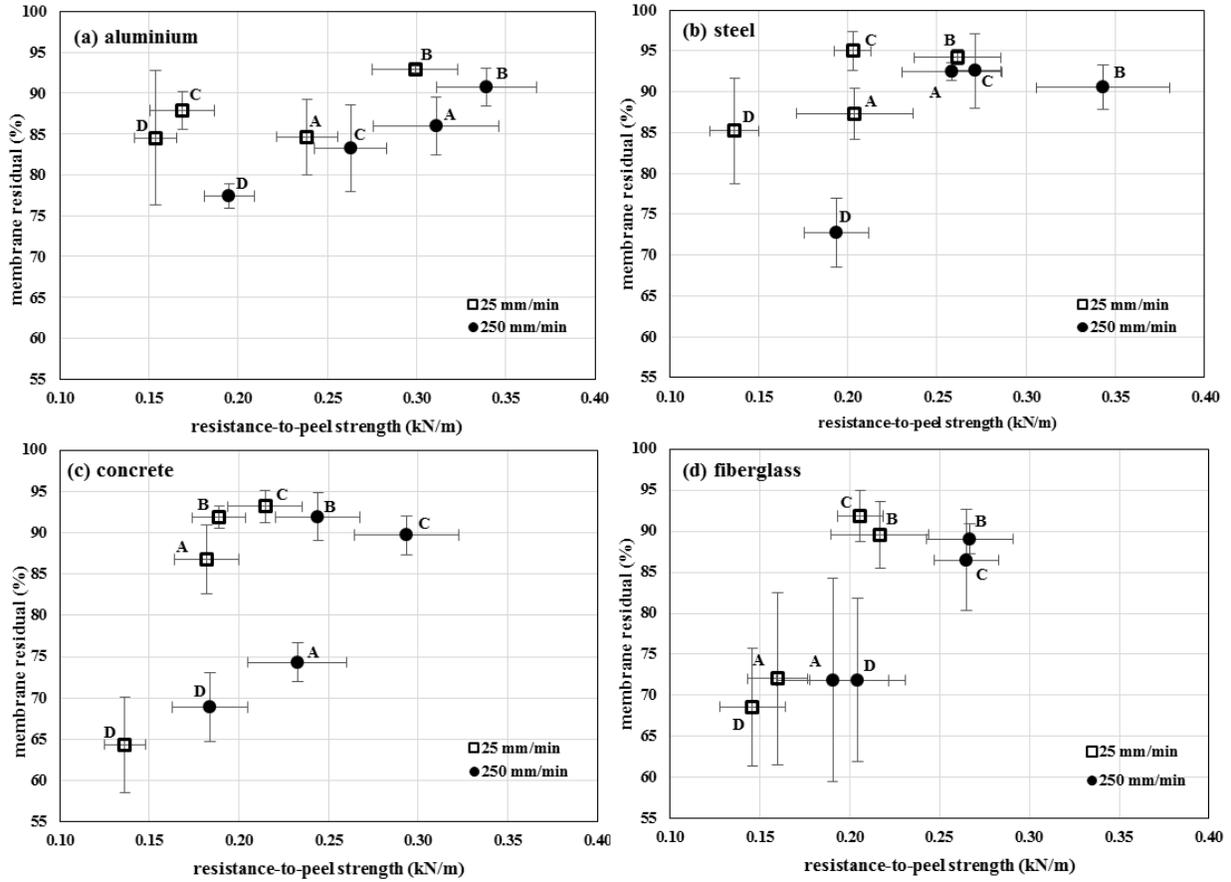
Figure 7 The residual percentage of membranes as a function of the peel resistance of four adhesives on (a) aluminium; (b) steel; (c) concrete; and (d) fiberglass; "A", "B", "C", and "D" stand for adhesives A, B, C and D, respectively.

Figure 8 compares the membrane residuals for two extreme examples, namely, two samples using adhesives adhesive B and adhesive D, respectively, on a concrete substrate as a function of the peel resistance with corresponding post-peel areas at a peeling rate of 250 mm/min. Figure 8(a) shows that the post-peel residual percentage of the adhesive B adhered membrane (88%) is significantly higher than that of the adhesive D adhered membrane (78%), consistent with a higher peel resistance (0.249 kN/m) than that of the adhesive D sample (0.173 kN/m). Figure 8(b) shows pictures of the post-peel surface of both samples. The peeled area of the sample using adhesive B exhibits a few concentrated regions without residuals. However, the sample using adhesive D exhibits uniformly dispersed no residual areas from adhesion failure [23], possibly explaining the inferior bonding performance of adhesive D.
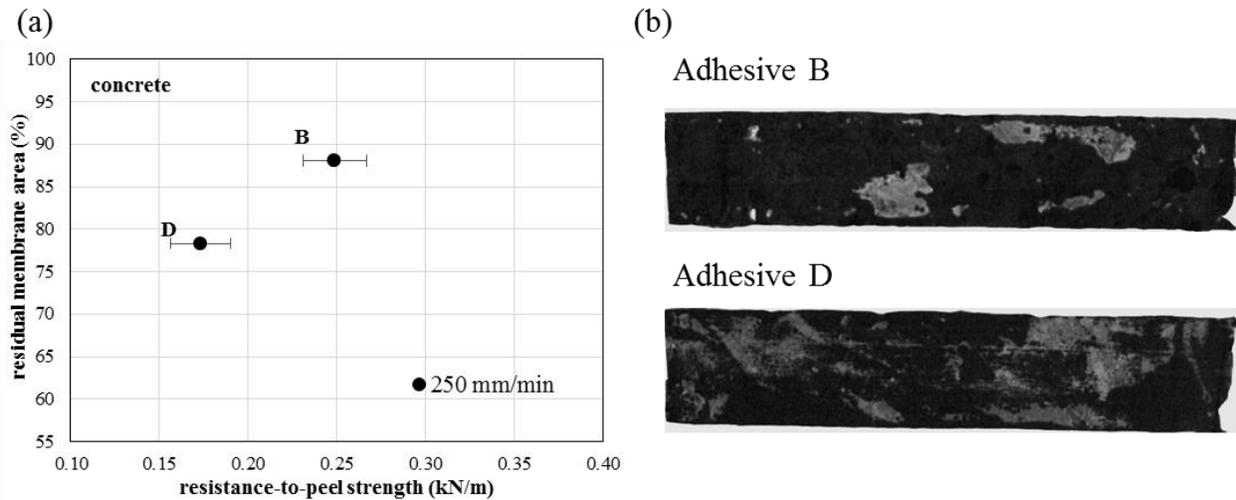
Figure 8(a) Residual percentage of two individual strip samples (adhesive B and adhesive D) on a concrete substrate as a function of the peel resistance with (b) corresponding post-peel areas at a peeling rate of 250 mm/min.

Conclusion

The peel resistance of four adhesives on common structural materials was investigated to study their applicability in large-scale deployment of a sensing membrane for SHM of mesosystems. The membrane layer adhering to the adhesive is an SEBS-CB composite. The adhesives under study consisted of adhesive A, adhesive B, adhesive C, and adhesive D. The structural material substrates were aluminium, steel, concrete, and fiberglass. Adhesive B exhibited the highest peel resistance on aluminium, steel, and fiberglass substrates, and adhesive C showed the highest strength on concrete. A cost analysis revealed that adhesive C was substantially more cost-effective compared to the other adhesives. The relationship between the peel resistance and the post-peel membrane residual percentage was also investigated. Adhesive B shows the highest peel resistance corresponding to the highest residual percentage of membrane after peel tests. Adhesive C did not exhibit a positive correlation between the peel resistance and residual percentage relation. Lastly, membrane samples with adhesive D exhibited major regions of adhesive failure, resulting in an inferior bonding performance on all substrates studied.

Acknowledgements

References

[1] Harms T., Sedigh S., Bastianini F., Structural health monitoring of bridges using wireless sensor networks, IEEE Instrum. Meas. Mag., 13 (2010) 14-8.

[2] Yu Y., Zhao X.F., Wang Y., Ou J.P., A study on PVDF sensor using wireless experimental system for bridge structural local monitoring, Telecommun. Syst., 52 (2013) 2357-66.

[3] LeBlanc B., Niezrecki C., Avitabile P., Chen J., Sherwood J., Damage detection and full surface characterization of a wind turbine blade using three-dimensional digital image correlation, Struct. Health Monit., 12 (2013) 430-9.

[4] Arsenault T.J., Achuthan A., Marzocca P., Grappasonni C., Coppotelli G., Development of a FBG based distributed strain sensor system for wind turbine structural health monitoring, Smart Mater. Struct., 22 (2013).

[5] Swartz R.A., Lynch J.P., Zerbst S., Sweetman B., Rolfes R., Structural monitoring of wind turbines using wireless sensor networks, Smart. Struct. Syst., 6 (2010) 183-96.

[6] Staszewski W.J., Mahzan S., Traynor R., Health monitoring of aerospace composite structures - Active and passive approach, Compos. Sci. Technol., 69 (2009) 1678-85.

[7] Tata U., Deshmukh S., Chiao J.C., Carter R., Huang H., Bio-inspired sensor skins for structural health monitoring, Smart Materials & Structures, 18 (2009).

[8] Mohammad I., Huang H., Monitoring fatigue crack growth and opening using antenna sensors, Smart Materials & Structures, 19 (2010).

[9] Jang S.D., Kim J., Passive wireless structural health monitoring sensor made with a flexible planar dipole antenna, Smart Mater. Struct., 21 (2012).

[10] Gao L.M., Thostenson E.T., Zhang Z.G., Byun J.H., Chou T.W., Damage monitoring in fiber-reinforced composites under fatigue loading using carbon nanotube networks, Philos. Mag., 90 (2010) 4085-99.

[11] Laflamme S., Saleem H.S., Vasan B.K., Geiger R.L., Chen D.G., Kessler M.R., et al., Soft elastomeric capacitor network for strain sensing over large surfaces, IEEE-ASME Trans. Mechatron., 18 (2013) 1647-54.

[12] Laflamme S., Kollosche M., Connor J.J., Kofod G., Robust flexible capacitive surface sensor for structural health monitoring applications, Journal of Engineering Mechanics, 139 (2013) 879-85.

[13] Higgins A., Adhesive bonding of aircraft structures, Int. J. Adhes. Adhes., 20 (2000) 367-76.

[14] Carbas R.J.C., da Silva L.F.M., Critchlow G.W., Adhesively bonded functionally graded joints by induction heating, Int. J. Adhes. Adhes., 48 (2014) 110-8.

[15] Wang L., Shui X.X., Zheng X., You J.C., Li Y.J., Investigations on the morphologies and properties of epoxy/acrylic rubber/nanoclay nanocomposites for adhesive films, Compos. Sci. Technol., 93 (2014) 46-53.

[16] da Silva L.F.M., D Adams R., Techniques to reduce the peel stresses in adhesive joints with composites, Int. J. Adhes. Adhes., 27 (2007) 227-35.

[17] Taljsten B., Strengthening of beams by plate bonding, J. Mater. Civ. Eng., 9 (1997) 206-12.

[18] Bascom W.D., Cottington R.L., Jones R.L., Peyser P., Fracture of epoxy-modified and elastomer-modified epoxy polymers in bulk and as adhesives, J. Appl. Polym. Sci., 19 (1975) 2545-62.

[19] deGennes P.G., Soft adhesives, Langmuir, 12 (1996) 4497-500.

[20] Gledhill R.A., Kinloch A.J., Yamini S., Young R.J., Relationship between mechanical-properties of and crack propogation in epoxy-resin adhesives, Polymer, 19 (1978) 574-82.

[21] Hong H.P., Jung K.H., Min N.K., Rhee Y.H., Park C.W., Ieee, A highly fast capacitive-type humidity sensor using percolating carbon nanotube films as a porous electrode material, 2012 Ieee Sensors Proceedings, 2012, pp. 410-3.

[22] Saleem H., Laflamme S., Ubertini F., Dynamic characterization of a soft elastomeric capacitor for structural health monitoring, SPIE Proceedings, 9061 (2014) 906115.
[23] Adhesives – designation of main failure patterns, International Standard, ISO10365-1992.
[24] Standard test methods for measuring adhesion by tape test, ASTM Standards, D3359-09 8.